

PAPER • OPEN ACCESS

Using Hyperspectral Frame Images from Unmanned Airborne Vehicle for Detailed Measurement of Boreal Forest 3D Structure

Recent citations

- [Lake Imaging and Monitoring Aerial Drone](#)
Jean-Luc Liardon *et al*

To cite this article: Raquel A. de Oliveira *et al* 2016 *IOP Conf. Ser.: Earth Environ. Sci.* **44** 042029

View the [article online](#) for updates and enhancements.



IOP | ebooks™

Bringing you innovative digital publishing with leading voices to create your essential collection of books in STEM research.

Start exploring the collection - download the first chapter of every title for free.

Using Hyperspectral Frame Images from Unmanned Airborne Vehicle for Detailed Measurement of Boreal Forest 3D Structure

Raquel A. de Oliveira ¹, Antonio M. G. Tommaselli ¹, Eija Honkavaara ²

¹ Univ Estadual Paulista, Department of Cartography, Roberto Simonsen 305, 19060-900 - Presidente Prudente, SP Brazil

² Finnish Geospatial Research Institute FGI, Geodeetinrinne 2 FI-02430 Masala, Finland

E-mail address: r.alvoliveira@gmail.com

Abstract. Objective of this work was to investigate the feasibility of using multi-image matching and information extracted from image classification to improve strategies in generation of point clouds of 3D forest scene. Image data sets were collected by a Fabry-Pérot interferometer (FPI) based hyperspectral frame camera on-board a UAV in a boreal forest area. The results of the new method are analysed and compared with commercial software and LiDAR data. Experiments showed that the point clouds generated with the proposed algorithm fitted better with the LiDAR data at the ground level, which is favourable for digital terrain model (DTM) extraction.

1. Introduction

3D point clouds of forest areas are being increasingly used as a complementary data for several forestry applications, such as estimation of forest biomass, volume, disturbance and change. LiDAR point clouds usually have two or more pulse returns associated with the same emitted pulse and some pulses can penetrate below the canopy [1]. Due to this feature, they can be separated at ground and above-ground points, being feasible for the generation of digital terrain models (DTM) and canopy height models (CHM). Acquisition of points under the canopy by optical images and photogrammetric techniques depends on the visibility of the ground or bare soil in the images; as the point clouds generation from images is based on stereoscopy and image matching, the same point should be visible at least from two images [2]. With the miniaturization of hyperspectral sensors, cameras operable from small UAV have become available. The new hyperspectral imaging technologies based on frame cameras are becoming attractive alternatives to hyperspectral pushbroom sensors [3]. Integration of spectral information with the point clouds can provide several important advantages [4, 5].

Point clouds generation using optical images is based on image matching methods, such as area-based methods [6], global methods or semi-global methods [7]. Area-based methods use a similarity function that compares the intensity values of pixels in a local neighbourhood and, as a consequence, assumes that the neighboring pixels have same depth as the centre pixel. As noted by Kanade and Okutomi [6], when the correlation window is too small and does not have enough intensity variations, the quality of the correspondence estimation is affected because of the low signal/noise ratio. On the



other hand, when the windows are larger, covering a region with suitable grey level gradient, the position of the matched point may not be true if there are unaccounted depth variations in the matched area.

The utilization of the spectral information in matching process is an interesting possibility with novel imaging systems occupying multi- or hyperspectral frame sensors, but is rarely utilized.

This investigation studies image matching in forested scenes. Basically, forest objects can be separated into trees, shrubs and ground (if the forest is not highly dense). The forests can be grouped from sparse to dense depending on the tree density. Boreal forests present often sparse trees, allowing the visibility of bare soil in many areas when viewed from aerial or orbital images. The objective of this work is to investigate the feasibility of using spectral information in forest generation. Here the focus is to study its potential in optimizing the selection of the parameters of matching techniques (window size, search space, similarity threshold) for different objects (ground and tree tops) in an object space-based multi-image matching approach.

2. Proposed methodology for point cloud generation

This work uses vertical line locus (VLL) method that is an object based reconstruction algorithm [8]. Assuming that the EOPs of each image and the approximate heights (Z_0) of the area are known, the main steps of the image matching process are: (1) Maximum and minimum values are established ($Z_{max} = Z_0 + \Delta Z_{max}$ and $Z_{min} = Z_0 - \Delta Z_{min}$) to bound the vertical line search range of a point P. A height increment (dZ) is defined; (2) The photogrammetric coordinates of P are calculated for each image in which the point appears, using the collinearity equations and $Z_i = Z_{min} + (i * dZ)$, where $i=0$ to $(Z_{max} - Z_{min})/dZ$; windows are defined taking these image coordinates as the centre; (3) The correlation coefficient is used to calculate the similarity between the reference image (most nadir) and target images. The average of the coefficients higher than a threshold is taken as the Z_i score; (4) The height Z_i having the best similarity value between the windows, is selected as the estimated height for P.

At the highest resolution level of the hierarchic matching process, with full resolution images, the parameters (window size, vertical range, average height and thresholds) for the pixel under analysis change according to the class in the reference image. Computing correlation coefficients of templates with different sizes along the vertical line would lead to heterogeneous correlation scores for all the elevations and could lead to false matches. Thus, this strategy is used only at the highest resolution level selecting the parameters based on the approximated height from the previous level, which is already a better approximation than the first levels. Then the strategy keeps the same for all steps (dZ) in the vertical line.

3. Materials and methods

3.1. Study area and data set

The test area was located in Vesijako, Finland (N61°21'40", E25°6'4"). The primary tree species in the image block area was Birch (*Betula pendula*). The average tree height was approximately 21 m. The data capture was carried out on 26 June 2014 using a Tarot 960 hexacopter and during the full-leaf season. In this study the novel hyperspectral frame camera based on Fabry-Pérot interferometer (FPI) camera, prototype 2012b, was used [3, 9]. This camera acquires frame images with a rigid geometry, which allows the generation of 3D hyperspectral. However, bands are acquired in a sequential process, and as a consequence, the bands of an individual data cube are not co-registered. An image block with six image strips and 97 hyperspectral data cubes was captured at the flight height of 88 m above ground level; at tree tops the object distance was in average 67 m. The average ground sample distances (GSD) were from 6.7 to 8.8 cm and the forward and side overlaps were 65% and 57% at ground level. The flight speed was 4.6 m/s; the resulting distance of the first and last exposures of a single cube was 8.3 m (124 pixels at tree tops and 92 pixels on ground).

LiDAR data from the National Land Surveying of Finland acquired in 13 May 2012, with an approximate point density of 1 points per 2 m² was used as the reference DTM (<http://www.maanmittauslaitos.fi/en/digituotteet/laser-scanning-data>).

3.2. Photogrammetric processing

Exterior Orientation of the images and a point cloud were determined using Agisoft PhotoScan Professional commercial software. The FPI block structure with relatively low overlaps was not ideal for the PhotoScan processing since its algorithm is based on structure-from-motion (SfM) technique requiring small baselines (high overlap with many images). To obtain better overlaps, three bands of each cube were used as independent images since each image band is displaced with respect to the others of the same cube due to the camera movement during acquisition (in this flight configuration 5-124 pixels at tree tops). In PhotoScan project the initial values for camera position were based on the data collected by an on-board navigation grade GNSS receiver; attitude angles were considered as unknowns; IOPs were based on the nominal values and inserted as approximate values to be estimated during the bundle adjustment (on the job calibration); four signalled ground control points (GCP) were used; tie points were automatically generated using maximum of 40000 points per model. The PhotoScan software was also used to generate a dense point cloud of the test area. The dense reconstruction was performed using “ultra-high resolution” option. A re-projection error of 0.7 pixels was achieved and it could see good fit of the point cloud with the reference LiDAR data.

3.3. Point cloud generation using multi image VLL with classified images

From the full image block area, a smaller area of 60 m x 60 m with ten data cubes was selected as the test area. First, the cubes were co-registered taking one of the bands with estimated EOP as reference. The cubes were then classified using the k-means method, with 10 iterations, 0.95 convergence threshold, and four classes defined based on the forest characteristics. (ground-shadow, ground-vegetation, top of the trees and area between top and ground). Several classification techniques were tested, but k-means presented the best results for this case. The setups using one single band of each cube were used to perform the experiments. The test area represented typical boreal managed forest site where the ground was visible between trees.

4. Results

4.1. Results of point cloud generation

Results of classification with k-means algorithm are presented for one cube in Figure 1(a, b). The classification was considered suitable for the application; “ground-vegetation” class was in some cases associated as part of class “tree”, thus the vertical line length was assumed one meter higher than for the class “ground-shadow”. The proposed algorithm was run hierarchically using four levels. For the full resolution images, the matching parameters were selected on the basis of the image classification. Two point clouds were generated with the algorithm: with (CVLL) and without (OVLL) the parameters selection based on classified images. When using CVLL (full resolution level), the matching parameters were different according each class. Window size, for instance, was 11x11 pixels for classes “tree” and “tree top”; 17x17 pixels for class “ground-vegetation” and 21x21 pixels for class “ground-shadow”. However, with OVLL a correlation window with size of 11x11 pixels was used for all points. The visual analyzes of the generated point clouds with (Figure 1 (e)) and without classes (Figure 1 (f)) showed that the constraint applied to the matching based on the object classification have produced more points at the ground level while reducing the amount of outliers.

4.2. Comparison of point clouds generated with different techniques

The full LiDAR data (trees and ground) was resampled to a grid of 15x15 cm (Figure 1 (c)). The same was done with PhotoScan point cloud (Figure 1 (d)) and point clouds generated with the proposed algorithm (Figure 1 (e) CVLL, and (f) OVLL). It can be noted that, at the ground level, the CVLL method was the most similar with the LiDAR point cloud. PhotoScan performed well in the largest clearance areas. Figure 1 (g) shows profiles of the point clouds generated with PhotoScan, with the proposed technique and the LiDAR DTM. It can be noted that fewer spurious points were generated in

clearance areas with the proposed method. This means that the a priori classification and the generated parameters helped to avoid false matches. However, since forest gaps are usually more homogenous and have poorer dynamic range and lower image quality due to the presence of shadows (and reduced amount of illumination) there are still false matches. Point cloud ground and above-ground classification had also benefited with the proposed method, as it can be seen in Figure 1 (h) and (j), which presents the classified point cloud generated with CVLL. In addition, since hyperspectral images are being used, each point of the point cloud can recover the spectral information of each band (Figure 1 (i) and (l)).

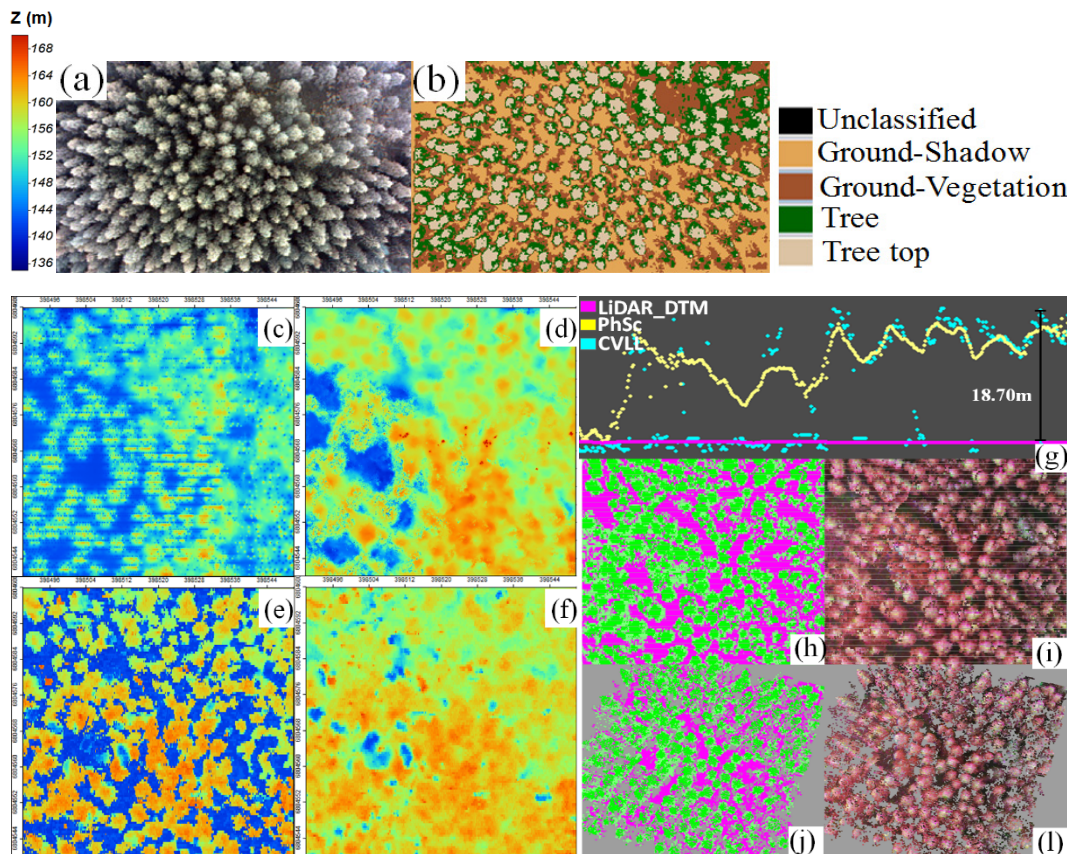


Figure 1. Results of the experiments. (a) FPI image (RGB composition); (b) Classified cube using k-means. Point clouds using (c) LiDAR data, (d) PhotoScan, (e) CVLL and (f) OVLL, (g) point clouds and LiDAR-DTM profiles overlaid. (h) and (i) Classified point cloud generated with CVLL; (j) and (l) CVLL colored with NIR-R-G

5. Conclusions

The results of this work showed that the simultaneous correspondence of multiple images constrained by classification enables optimization of the image based point cloud generation methods. Furthermore, they allow development of all-in-one matching methods providing both 3D object surface and spectral information. For example, when operating these methods from small UAV platforms they will provide powerful object characterizing tools that are useful in wide variety of earth measurement problems. At best, the quality of image matching based point clouds are with similar quality to those obtained by LiDAR data and with high information density. The generated point clouds showed that the utilization of classification information to guide the algorithm in determining the matching parameters provided better quality of points over bare soil. On the other hand, it also spurious points due to classification errors appeared, thus the feasible classification methods for different cases needs to be elaborated. The regions that present a challenge to the image matching, such as homogeneous areas deserve more studies. Also, the use of more bands during the image matching should be studied.

Acknowledgments

The authors would like to thank the FAPESP (grant n. 2013/14444-0) and the Academy of Finland (Decision number 273806) for funding of this project. Authors acknowledge Teemu Hakala and Niko Viljanen for capturing the UAV data sets.

References

- [1] Hyypä, J. et al., 2008. Review of methods of small-footprint airborne laser scanning for extracting forest inventory data in boreal forests. *Remote Sensing*, 29: 1339–1366
- [2] Baltsavias, E.; Gruen, A.; Zhang, L.; Waser, L.T., 2008. High quality image matching and automated generation of 3D tree models. *International Journal of Remote Sensing*, 29: 1243–1259
- [3] Honkavaara, E.; Saari, H.; Kaivosoja, J.; Polonen, I.; Hakala, T.; Litkey, P.; Makynen, J.; Pesonen, L., 2013. Processing and Assessment of Spectrometric, Stereoscopic Imagery Collected Using a Lightweight UAV Spectral Camera for Precision Agriculture. *Remote Sensing*, 5 (10): 5006–5039
- [4] Aasen, H., Burkart, A., Bolten, A., Bareth, G, 2015. Generating 3D hyperspectral information with lightweight UAV snapshot cameras for vegetation monitoring: from camera calibration to quality assurance. *ISPRS Journal of Photogrammetry and Remote Sensing*, 108, 245–259.
- [5] Näsi, R., Honkavaara, E., Lyytikäinen-Saarenmaa, P., Blomqvist, M., Litkey, P., Hakala, T., Viljanen, N., Kantola, T., Tanhuanpää, T., Holopainen, M., 2015. Using UAV-based photogrammetry and hyperspectral imaging for mapping bark beetle damage at tree-level. *Remote Sensing*, 7(11): 15467–15493
- [6] Kanade, T., Okutomi, M., 1991. A stereo matching algorithm with an adaptive window: Theory and experiments. In *Proceedings of IEEE International Conference on Robotics and Automation*, California, 1088-1095
- [7] Hirschmüller, H., 2005. Accurate and efficient stereo processing by semi-global matching and mutual information. *Proceedings of IEEE Conference on Computer Vision and Pattern Recognition*, 2005, San Diego, USA. San Diego: ICCVPR, 2: 807-814.
- [8] Paparoditis, N.; Polidori, L., (2003). DSM quality: internal and external validation. In: EGELS, Y.; Kasser, M. *Digital Photogrammetry*. New York: Taylor & Francis, 351p
- [9] Oliveira, R. A.; Tommaselli, A. M. G.; Honkavaara, E. (2016). Geometric calibration of a hyperspectral frame camera. *The Photogrammetric Record*.